Dynamical thresholds for the existence of excited electronic states of fast ions in solids

Jörg Müller and Joachim Burgdörfer
Department of Physics, University of Tennessee, Knoxville, Tennessee 37996-1200
and Oak Ridge National Laboratory, Oak Ridge, Tennessee 37831-6377
(Received 30 November 1990)

We calculate eigenenergies for bound states of electrons in the dynamical screening potential of a fast charged particle traversing a solid by diagonalization of Hamiltonian matrices in a truncated Hilbert space of 600 hydrogenic basis states. Application of classical scaling invariances yields a universal energy-level diagram. A simple approximate formula for projectile-centered one-electron bound states is obtained. We find velocity thresholds for the existence of excited states which are in surprisingly good agreement with recent data by Chevallier et al. [Phys. Rev. A **41**, 1738 (1990)].

The formation and evolution of bound states of fast charged particles penetrating solids are of continuing interest and a subject of intensive investigations.[1-3] One fundamental problem is that of their existence inside the solid, in particular, for excited states. The propagation of the projectile with speed $v_p \gg v_F$ (v_F is the Fermi velocity) in a dense medium leads to a strong perturbation of atomic states which has, until now, prevented the accurate determination of the projectile spectrum. The complication results from two processes which are, in fact, closely related to each other. The interaction with the medium, the ionic cores of the target as well as the delocalized valence electrons, causes collisional destruction and broadening of all levels. Therefore, projectile-centered states will be, at best, quasibound states due to collisional ionization. Secondly, the collective response of the medium, in particular of the quasi-free valence (or conduction) electrons, leads to dynamical screening of the ionic potential of the projectile. Even in the absence of collisions the atomic or ionic spectra of the projectile are therefore strongly distorted. Since the screened potential is short ranged only a finite number of such quasibound states may exist. Rogers, Graboske, and Harwood[4] performed a systematic study of the hydrogenic spectra in the limit of static ($v_p \to 0$) isotropic Debye-type screening. They concluded that the number of bound states will be drastically reduced, in particular that protons ($Q = 1$) do not possess a bound state in an electron gas of solid-state density.

For fast projectiles ($v_p > v_F$) the modification of the hydrogenic spectrum is determined by the dynamical[5] rather than static screening. The motion of a fast charged particle through a solid polarizes the medium which results in an anisotropic enhancement of electron density behind the projectile ("wake"). The enhancement of electron density leads to an electric field which will result in Stark splitting of bound states of the projectile. Since the effectiveness of screening is projectile-velocity dependent it was suggested some time ago[2,6] that "critical " threshold velocities should exist below which a given projectile state enters the continuum and ceases to exist as a quasi-

bound state. Only recently, Chevallier et al.[7] found the first experimental evidence for a dynamical threshold for the $n = 3$ manifold.

In the following we present a study of the nonrelativistic bound-state spectrum of a hydrogenic ion with charge Q in the presence of a dynamical screening potential. The conduction electrons are represented by an electron gas. We find simple scaling properties of the spectrum of this system if we neglect the non-Hermitian part of the Hamiltonian due to collisional decay as well as crystal-field effects. We will then discuss the size of collision-induced level broadening. Using a simple approximation for the non-Hermitian part, we find only small shifts in the positions of the resonances, i.e., the real part of the eigenvalues. Furthermore, we find critical velocities for each manifold whose exact position are, however, smeared out due to collisional broadening.

The static crystal potential has not been included in this work, since it depends on the orientation of the beam relatively to the crystallographic axis. The error due to the neglect of the crystal-field effects is largest for highly excited states with extended wave functions. However, in this regime collisional broadening due to scattering of the projectile electron at the target-ion cores will lead to overlapping resonances and thus make the identification of individual states impossible. We furthermore neglect the dynamic response of the target cores. The latter is expected to be most important for highly charged ions.

The nonrelativistic Hamiltonian of an electron in the dynamical screening potential is given in a.u. by [5]

$$H = \frac{p^2}{2} + V_{sc}(\rho, z),$$ (1)

where V_{sc} is the dynamical screening potential that is in linear approximation given by

$$V_{sc}(z,\rho) = \frac{Q}{\pi v_p} \int_{-\infty}^{\infty} d\omega \int_{0}^{\infty} \kappa \, d\kappa \frac{J_0(\rho \kappa) \exp(-i\omega z / v_P)}{(\kappa^2 + \omega^2 / v_p^2) \epsilon(q, \omega)} .$$

(2)

The speed of the projectile is denoted by v_p and its charge by Q, z, and ρ are cylindrical coordinates in the frame of the projectile, q is the wave number, and $\kappa = (q^2 - \omega^2/v_p^2)^{1/2}$. The linear response underlying (2) is valid for $Q/v_p \ll 1$, i.e., for small Sommerfeld parameters for Coulomb scattering of the electron gas at the projectile. For the dielectric function $\epsilon(q,\omega)$ in (2) we chose the plasmon pole approximation[5,8-10] which, in spite of its simplicity, represents important features of the dynamical screening quite well. Using this approximation the integral over ω can be performed, but the potential is still given in terms of a one-dimensional numerical integral. The Hamiltonian possesses rotation symmetry about the beam $(\hat{z})$ axis. In the nonrelativistic problem the orbital angular momentum L_z with exact quantum number m is therefore conserved. Approximate energy eigenvalues of (1) can be found in a straightforward fashion by expanding the trial wave function ψ_{im} for the ith eigenstate in a suitable basis

$$\psi_{im} = \sum_{nl} C_{nlm}^{(i)} \phi_{nlm}. \tag{3}$$

Relativistic corrections have been neglected in (1) and (3) but can be included if necessary for high Q. We have used a hydrogenic basis with basis size for given m of ≈ 600. The expansion (3) converts the Schrödinger equation into a 600×600 matrix eigenvalue equation for the Hamiltonian matrix $\langle nlm | H | n'l'm \rangle$ that can be solved by diag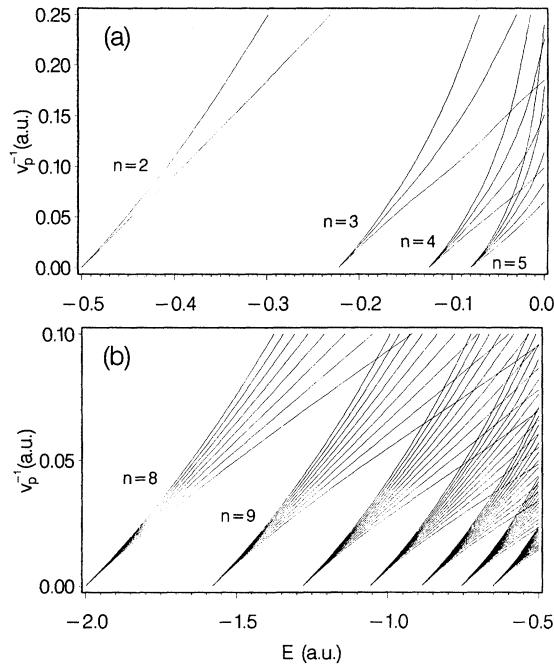onalization. We have tested the convergence as a function of the basis size. Convergence could possibly be accelerated by using a Sturmian[11] rather than a hydrogenic basis.

Figure 1 displays the $m = 0$, $n = 2$, 3, 4, and 5 manifolds of He$^+$ in (a) carbon and the $m = 0$, $n = 8$ to 14 manifolds of S^{15+} in (b) gold as a function of v_p^{-1}. The effect of the perturbation vanishes in the limit $v_p \to \infty$ (or $v_p^{-1} \to 0$), since the dynamical screening length

$$\lambda_D = v_p / \omega_p \tag{4}$$

becomes large compared to the extent of the wave function of the bound states. The extrapolation of the energy levels shifted to the ionization limit $(E = 0)$ determines the threshold velocity, v_c for the existence of a given (quasi) bound state. It should be noted that the spectrum becomes complicated near threshold due to a multitude of avoided crossings with only weakly shifted levels from higher manifolds. Near the ionization limit it is thus impossible to keep track of the "identity" of the shifted energy levels. We use, therefore, simply the diabatic extrapolation of the energy levels (by replacing all avoided crossings by crossings) to determine the approximate thresholds. The application of diabatic extrapolation is justified in the energy regime associated with classically regular motion[10] $(E < -Q^2 \omega_p / 20 v_p)$ since the wave functions retain their character through an isolated avoided crossing, characteristic for regular motion. Close to threshold the classical motion becomes chaotic.[10] The large number of overlapping avoided crossings characteristic for chaotic motion introduces, however, little uncertainty with respect to the critical velocity v_c, since collisional broadening of the energy levels exceeds the width of this chaotic spectral region for not too large charges Q.

In principle, this large-scale diagonalization method has to be applied for each charge state Q, each quantum number m, each projectile velocity, and each target. The latter is characterized by its plasmon frequency ω_p (or electron density N_e, $\omega_p = \sqrt{4\pi N_e}$). The similarity of the energy-level diagram for different n manifolds, different projectiles, and different targets (Fig. 1) suggests, however, the existence of an underlying universal energy-level pattern. We note that such a universal level diagram exists only for the classically regular regime. In the weak perturbation limit $(v_p^{-1} \to 0)$, each manifold displays a Stark splitting determined by the electric quantum number k. In this limit the eigenstates (3) are approximate Stark states. The Stark splitting of low-lying energy levels in the solid has been observed in resonant coherent excitation of the $n = 2$ manifold[12] and the Stark "beats" in the substate population[13] of highly charged ions. In the regime of strong perturbation we will continue to use the state label k even though the eigenstates are no longer Stark states.

To uncover the universal energy-level diagram we invoke classical scaling invariances[10] for this problem. Since classical dynamics, unlike quantum mechanics (via $\hbar$), does not possess a fundamental scale, the classical equations of motion are invariant under mechanical similarity transformations. We have found for this problem

FIG. 1. Energy-level diagram (a) for the $m = 0$, $n = 2$ to $n = 5$ manifolds of He$^+$ in carbon ($\omega_p = 0.81$) and (b) for the $m = 0$, $n = 8$ to $n = 14$ manifolds of S^{15+} ($\omega_p = 0.33$) in gold, as a function of v_p^{-1}, $k = (n-1)$, $(n-3)$, ..., $(-n+1)$ from top to bottom.

TABLE I. Classical scaling invariances for the dynamical screening potential. Scaling transformations with scaling variables $\alpha,\beta,\gamma, > 0$. Q is the charge of projectile, v_p is the velocity of projectile, ω_p is the plasmon frequency of the medium (foil), E is the energy separation of the electron, S is the classical action, t is time, p is the momentum of the electron, and q represents the coordinates (ρ and z) of the electron.

Transformation I (exact)	Transformation II (approximate)	Transformation III (approximate)
$Q'=\alpha Q$	$Q'=Q$	$Q'=Q$
$v_p'=v_p$	$v_p'=\beta v_p$	$v_p'=\gamma v_p$
$\omega_p'=\omega_p$	$\omega_p'=\beta\omega_p$	$\omega_p'=\omega_p$
$E'=\alpha E$	$E'=E$	$E'=1/\gamma E$
$S'=\sqrt{\alpha}S$	$S'=S$	$S'=\gamma^{1/2}S$
$t'=(1/\sqrt{\alpha})t$	$t'=t$	$t'=\gamma^{3/2}t$
$p'=\sqrt{\alpha}p$	$p'=p$	$p'=\gamma^{-1/2}p$
$q'=q$	$q'=q$	$q'=\gamma q$

three invariant scaling transformations (Table I), one of which is exact while the others are valid to a good degree of approximation. Note that only transformation II involves target variables and may be altered for different choices of the dielectric function, in particular if $\epsilon(q,\omega)$ depends on additional characteristic parameters besides ω_p. Transformation III is the scaling transformation of the Kepler problem and becomes invalid at large distances when dynamical screening dominates. The application of classical scaling invariances to the quantal energy spectrum derives its justification from the correspondence principle.[14] The energy-level spectrum should satisfy classical scaling invariances in the quasiclassical limit of large quantum numbers. In the present case the justification of classical scaling invariances, both exact and approximate, is *a posteriori*. We show explicitly that the numerically calculated eigenvalues satisfy, to a good degree of approximation, the scaling invariances. To this end we use the following scaling parameters:

$$\alpha=Q^{-1}, \tag{5}$$

$$\beta=(\pi\omega_p)^{-1}, \tag{6}$$

$$\gamma=Q/n^2. \tag{7}$$

These transformations rescale the unperturbed energy to that of the ground state of hydrogen ($E=-\frac{1}{2}$). Accordingly, scaled velocities are given by

$$\bar{v}=\frac{Q}{\pi\omega_p n^2}v, \tag{8}$$

and scaled energies by

$$\bar{E}=\frac{n^2}{Q^2}E. \tag{9}$$

Using a scaled electric quantum number $\bar{k}=k/n$ the calculated energy-level spectra for different Q, n, v_p, and ω_p can be mapped onto a scaled universal energy-level diagram (Fig. 2). The close agreement of different data sets attests to the validity of the scaling transformations for the quantum spectrum. We can furthermore find a simple analytic formula describing the $\bar{v}_p^{-1}$ dependence of the energy levels within the universal manifold. To this

end we map the scaled energy level onto the interval [0,1] via the transformation

$$\bar{\varepsilon}=2\bar{E}+1, \tag{10}$$

where $\bar{\varepsilon}=0$ corresponds to the unperturbed energy and $\bar{\varepsilon}=1$ corresponds to the ionization threshold. The energy-level curves can now be well represented by the formula

$$\bar{v}_p^{-1}=\bar{\varepsilon}-\bar{k}(\bar{\varepsilon}^2-\bar{\varepsilon}^3)+[\bar{v}_c^{-1}(\bar{k})-1]\bar{\varepsilon}^4. \tag{11}$$

The only fit parameter in (11), $\bar{v}_c^{-1}$, is the reciprocal of the scaled critical velocity. The latter can be parametrized in terms of the scaled electric quantum ($\bar{k}$) as

$$\bar{v}_c(\bar{k})=(0.81-0.36\bar{k})^2. \tag{12}$$

The deviation between the matrix diagonalization and the results obtained with Eq. (11) are generally less than 2% of the unperturbed energy. Transforming to the original physical variables we obtain
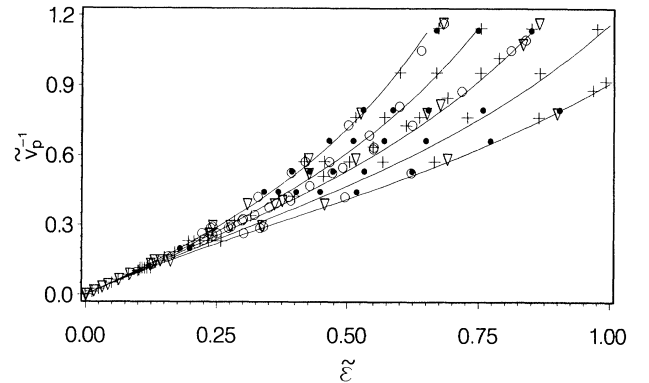

FIG. 2. Rescaled universal energy-level diagram for hydrogenic manifolds in an electron gas described by a dielectric function in the plasmon-pole approximation. Scaled electric quantum number $\bar{k}=\frac{2}{3},\frac{1}{3},0,-\frac{1}{3},-\frac{2}{3}$, from top to bottom; ——, Eq. (11). Results from numerical diagonalization [Eq. (1)]: +, $Q=2$, $\omega_p=0.81$; O, $Q=16$, $\omega_p=0.33$; ∇, $Q=2$, $\omega_p=0.33$; ●, $Q=8$, $\omega_p=0.56$.

$$v_p^{-1}(n,k,E,\omega_p,Q)$$

$$= \frac{Q}{n^2\omega_p\pi} + \frac{2E}{\pi\omega_p Q}\left[1 - \frac{k}{n}\left[\frac{2n^2}{Q^2}E+1\right]^2\right]$$

$$+ \left[\frac{1}{v_c} - \frac{Q}{n^2\omega_p\pi}\right]\left[\frac{2n^2}{Q^2}E+1\right]^4 \quad (13)$$

with the critical velocity $v_c = v_p(E=0)$

$$v_c(n,k,\omega_p,Q) = \frac{\omega_p}{Q}(1.43n - 0.64k)^2. \quad (14)$$

v_c describes the velocity at which a given state enters the positive-energy continuum. Equation (13) can be numerically inverted to give binding energies for a given choice of n, k, ω_p, Q, and v_p. A direct comparison of these energies with experimental data by Datz et al.[12] and calculations by Crawford and Ritchie,[15] who present transition energies ΔE from the $n=2$ manifold to the $1s$ ground state, is difficult due to the presence of crystal-field effects. However, an indirect comparison using the difference

$$\delta(v_p,Q,\omega_p,k) = \Delta E(v_p,Q,\omega_p,k) - \Delta E_\infty(Q,\omega_p,k)$$

[where $\Delta E_\infty(Q,\omega_p,k)$ is the transition energy in the limit $v_p \to \infty$, which for Ref. 15 includes the static crystal field] is possible. Generally we find good agreement. Deviations with Ref. 15 at very high projectile velocities can be attributed to the omission of the crystal field, which splits the energy levels within a given n manifold even in the limit $v_p \to \infty$. Here the crystal field leads to a quadratic rather than a linear Stark effect.

The threshold for a given n manifold can be defined by the critical velocity v_c ($k=n-1$), when the most stable state (with the largest value k) enters the continuum. Figure 3 shows the threshold line for n manifolds in carbon in the (Q,v_p) plane.

The comparison with the recent observation by Chevallier et al.[7] of a sudden change of the velocity dependence of the population ratio $P(\text{He}^+(3p))/P(\text{He}^+)$ after exiting the foil requires a mapping of states inside the
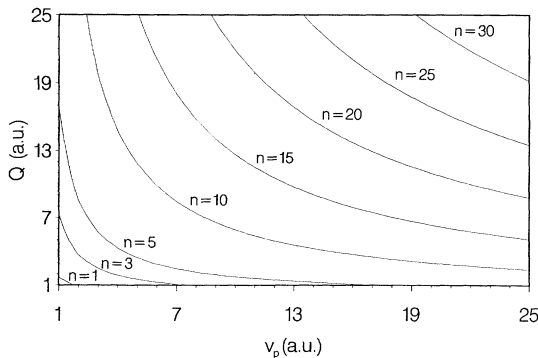
solid onto the asymptotic, field-free states for which we use a sudden approximation in view of the high projectile speed. We find the admixture of lower-lying manifolds to the $n=3$ He$^+$ states in vacuum to be less that 1%, which indicates that the threshold remains unchanged. We find an $n=3$ threshold of $v_c=3.6$ a.u. which is in amazing agreement with the experimental value of $v_c \simeq 3.7$ a.u. This agreement is expected to be, in part, fortuitous for several reasons: collisional broadening is expected to smear out any sharp threshold. The width is of the order of[3,16,17]

$$\Gamma_c = \frac{\omega_p\ln(\sqrt{2/\omega_p}v_p)}{v_p} + \frac{4\pi Z_T^2 N_T v_p}{\dfrac{v_p^2}{1.3Z_T^{2/3}} + \left[\dfrac{Q^2}{2n^2}\right]^2}, \quad (15)$$

where $Z_T = 6$ is the charge of the carbon nucleus and N_T is the target density. A typical value for the collisional broadening for this system is $\Gamma_c \approx 2.5v_p^{-1}$ a.u. The size of collisional broadening should prevent accurately defining a threshold value. Furthermore, it appears that experimental determination of sudden changes in the population of excited states is subject to considerable uncertainty due to cascade contributions and the obstruction of the signal near the foil.

The decay of states due to collisional destruction and photon emission can be taken into account in terms of a non-Hermitian contribution to the effective Hamiltonian. To this end we have performed numerical diagonalization of the non-Hermitian Hamiltonian which has Eq. (1) as Hermitian and $\Gamma_c/2$ as anti-Hermitian part. Our calculations for a few test cases show that the spectrum (Fig. 2), i.e., the real part of the complex eigenenergies is little affected (typically less than 0.1%) despite the large broadening which leads eventually to overlapping resonances near the ionization limit. The reason for the relative insensitivity is that the approximate decay rate [Eq. (15)] does not depend on the substate quantum numbers of a given manifold.

Finally, Eq. (11) can be solved for $\tilde{\epsilon}$ and, in turn, for E in terms of a power series in $x = n^2/Q\lambda_D$, the ratio of the radius of the excited state to screening length,

$$\tilde{\epsilon} = \sum_{s=0}^{\infty} a_s x^s. \quad (16)$$

To second order in x we find for large screening length (large v_p)

$$E(n,k,v_p,\omega_p,Q) \approx -\frac{Q^2}{2n^2} + \frac{\pi}{2}\frac{Q\omega_p}{v_p}$$

$$+ \frac{\pi^2}{2}kn\frac{\omega_p^2}{v_p^2} + O(v_p^{-3}). \quad (17)$$

The physical meaning of the individual terms is as follows: The first term corresponds to the unperturbed energy. The second term, which is proportional to v_p^{-1}, equals the dynamical screening potential at the position of the projectile and leads to a uniform state independent shift of the energy levels. This shift could account, in

FIG. 3. Threshold lines for different n manifolds in the (Q,v_p) plane (calculated for carbon, $\omega_p = 0.81$).

part, for the observed shift of the peak in the x-ray spectrum due to radiative electron capture (REC) recently observed by Vane et al.[18] for highly charged channeled ions. It should be noted that for highly charged ions dynamical screening by target cores may contribute to the energy shift as well. The third one, proportional to v_p^{-2}, is due to the linear Stark effect, which is proportional to the dynamical screening field, i.e., the derivative of the dynamical screening potential along the beam direction ($\bar{z}$) evaluated at the position of the projectile. This term can be compared with a first-order perturbation theory for the Stark effect using the electric field of the screening charge at the origin in plasmon-pole approximation.

$$\Delta E = \frac{3\ln(v_p/v_F)}{2}kn\frac{\omega_p^2}{v_p^2} . \tag{18}$$

Equation (18) agrees with the corresponding term of the series expansion up to a factor $\simeq \ln(v_p/v_F)/\pi$, which for $4 \le v_p/v_F \le 20$ varies between 0.46 and 1.

In summary, classical scaling invariances allow the determination of a simple analytic approximation formula for nonrelativistic hydrogenic energy levels in the presence of strong dynamical screening in an electron gas described by the dielectric function $\epsilon(k,\omega)$ in the plasmon-pole approximation. Predicted velocity-dependent thresholds for the existence of bound excited states in the medium agree with recent experiments. The presented results apply to situations where, on the average, at most one electron will be bound to the projectile.[3] Therefore the velocity of the projectile (in a.u.) is required to be larger than the charge of the projectile. Extrapolation to smaller speeds will only give qualitative trends of the behavior of the spectrum. The present calculation suffers from the uncertainties associated with the case of the plasmon-pole approximation to the dielectric function. The latter becomes important in particular when the linearity parameter Q/v_p is no longer small compared to 1. An analysis using an improved $\epsilon(k,\omega)$ in random-phase approximation is in progress.

[1]N. Bohr, K. Dan. Vidensk. Mat.-Fys. Medd. 18, No. 8 (1948); N. Bohr and J. Lindhard, ibid. 28, No. 7 (1954).

[2]W. Brandt, in Atomic Collisions in Solids, edited by S. Datz et al. (Plenum, New York, 1975), p. 247.

[3]J. Burgdörfer, in Proceedings of the Fourth Workshop on High-Energy Ion-Atom Collisions, edited by D. Berenyi and D. Hock, Notes in Physics (Springer, Berlin, in press), and references therein.

[4]F. Rogers, H. Graboske, and D. Harwood, Phys. Rev. A 1, 1577 (1970).

[5]J. Neufeld and R. H. Ritchie, Phys. Rev. 98, 1632 (1955); 99, 1125 (1955); P.M. Echenique, R. H. Ritchie, and W. Brandt, Phys. Rev. B 20, 2567 (1979).

[6]J. Burgdörfer, Diploma thesis, Freie Universtät Berlin, Berlin, Germany, 1978 (unpublished).

[7]M. Chevallier, A. Clouvas, N. De Castro Faria, B. Farizon Mazuy, M. Gaillard, J. Poizat, J. Remillieux, and J. Desequelles, Phys. Rev. A 41, 1738 (1990).

[8]A. Faibis, R. Kaim, I. Plesser, and Z. Vager, Nucl. Instrum. Methods 170, 99 (1980).

[9]A. Mazarro, P. M. Echenique, and R. H. Ritchie, Phys. Rev. B 27, 4117 (1983).

[10]J. Müller and J. Burgdörfer, Phys. Rev. A 41, 4903 (1990); J. Müller, J. Burgdörfer, D. W. Noid, in Proceedings of the Miniworkshop on Quantum Chaos, Trieste, Italy (World Scientific, Singapore, 1991); J. Müller, J. Burgdörfer, and D. W. Noid, Chem. Phys. Lett. 178, 60 (1991).

[11]M. Rotenberg, Ann. Phys. 14, 262 (1962).

[12]S. Datz et al., Phys. Rev. Lett. 40, 843 (1978); J. Phys. (Paris) Colloq. 40, C1-335 (1979).

[13]J. Rozet, A Chetioui, C. Stephan, A. Touati, D. Vernhet, and K. Wohrer, in Proceedings of the Third Workshop on High Energy Ion-Atom Collisions, edited by D. Berenyi and G. Hock, Lecture Notes in Physics Vol. 294 (Springer-Verlag, Berlin, 1988), p. 307.

[14]P. Koch, in Electronic and Atomic Collisions, edited by H. Gilbody, W. Newell, F. Read, and A. Smith (North-Holland, Amsterdam, 1988), p. 501.

[15]O. H. Crawford and R. H. Ritchie, Phys. Rev. A 20, 1848 (1979).

[16]P. M. Echenique, F. Flores, and R. H. Ritchie, Nucl. Instrum. Methods B 33, 911 (1988).

[17]D. Röschenthaler et al., J. Phys. B 16, L233 (1983).

[18]C. R. Vane et al. (private communication).